Analysis and Performance of a Grid-Connected PV System for Harmonic Compensation from Non-Linear Industrial Loads

Leonardo Teodosio da Costa[1], Washington Luiz Araújo Neves[1], Flávio Bezerra Costa[2], José Fábio Brilhante de Freitas Filho[1]

[1]Department of Electrical Engineering, Federal University of Campina Grande, Campina Grande, Brazil
[2]Department of Electrical and Computer Engineering, Michigan Technological University, MTU Houghton, United States of America

Email: [1]leonardo.costa@ee.ufcg.edu.br, [1]waneves@dee.ufcg.edu.br, [2]fbcosta@mtu.edu, [1]jose.brilhante@ee.ufcg.edu.br

Abstract- When non-linear loads are connected to the electrical system, several unwanted conditions are observed: voltage unbalance, voltage and current harmonic distortions and low power factor. This may compromise the stability of the electrical system. In this work, a compensation scheme, aiming to improve power quality (PQ), is proposed to reduce the total harmonic current distortion in a distributed generation (DG) system connected to the electrical grid. This compensation is performed by means of a three-phase inverter, whose DC bus is connected to the photovoltaic system, acting as an active power filter (APF). In this way, contributions from the control strategy used for the connection of photovoltaic systems are proposed, reducing the effects of non-linear loads, where the compensation is performed without the need to extract the harmonic components present in the current. Performing harmonic compensation at the point of common coupling (PCC) ensures that the electrical grid supplies or delivers only active power and the current has the lowest possible harmonic content. The control of the output currents is carried out indirectly and the power balance in the electrical grid and in the voltage inverter is carried out in the synchronous reference. The simulation results were performed using the MATLAB/SIMULINK ® software, validating the proposed control strategy and highlighting the harmonic compensation in the electrical grid.

Keywords— Compensation, Control, Harmonics, Non-Linear Load, Photovoltaic Systems.

I. INTRODUCTION

The generation of electric energy in Brazil is characterized by having a large hydroelectric matrix. As a result, due to water scarcity, and the need to minimize pollutants and increase investments in renewable energy sources, photovoltaic (PV) systems have gained increasing prominence in terms of installed capacity, contributing to the diversification of the Brazilian energy matrix. According to [1], the number of photovoltaic installations connected to the power grid in Brazil reached the mark of 816,061, totaling 8,877,697.35 kW of installed power in January 2022.

The insertion of distributed generation (DG) in the electrical grid allows maintaining the power quality (PQ), i.e, they ensure that power system operates safely and reliably. According to [2], disturbances that cause problems to PQ stand out, e.g, transients, short and long-term voltage variations, voltage distortions, frequency variation and among others. The presence of harmonics causes problems such as increased losses in electrical conductors, saturation, resonance, reduced life of transformers and malfunctions and operational failures in electronic equipment connected to grid [3]. These problems are greater in low voltage power grid due to the large amount of loads that produce harmonic current components [4]. In this case, the effects of distorted currents are aggravated the electrical grid has high impedance, causing voltage distortions. An alternative to minimize PQ problems is harmonic compensation, so that the DG works like an active power filter (APF).

The presence of non-linear loads connected to the point of common coupling (PCC) produces harmonic currents that degrade the PQ for all consumers connected to grid, APF is used to reduce harmonic components, compensating current harmonic components that circulate through the grid when added to the current drained by the non-linear load [5]. A non-linear load model, for example, can be represented by an electric arc furnace (EAF), which is among the largest loads that generate harmonics, unbalances and voltage fluctuations *(Flicker)*. The same is characterized by high variations in currents and voltages, causing disturbances to the grid. According to [6], converters have been used not only to inject active and reactive power, but as an APF, compensating harmonics components. Analyzed by [7], a single-phase photovoltaic converter performs reactive power and harmonics compensation, in addition to injecting active power into the grid. According to [8], harmonic compensation is performed based on a three-phase (PV) system connected to the grid.

This paper evaluates the performance and contributions from the control strategy used for the connection of photovoltaic systems are proposed, minimizing disturbances from non-linear loads, where the compensation is performed without the need to extract the harmonie components present in the current. As for the control strategy, it is performed so that the reference of the fundamental current is obtained by the bus control. The Proportional Resonant Current (PR) controller is presented and discussed by [9] and is based on the Park *(abc-dq)* and Clarke *(abc-αβ)* transformation [10]. Although this controller has a high ability to trace a sinusoidal reference, the output current of the grid-connected inverter is not immune to harmonic content. Therefore, the control strategy used in this work requires low computational complexity, since it does not require elements to extract harmonic components.

II. Structure Of PV System Connected To The Grid

With the presence of non-linear loads connected to the PCC, as in the case of EAF, the grid current is affected by harmonic distortions due to the non-linearities of the load. Some recommendations and international standards, such as IEEE-519 Std 1992 , IEEE 929 and *European IEC standards* IEC 61727 establish acceptable limits and levels regarding the insertion of harmonics in the grid [11-13]. The PV can act as a PAF by injecting harmonics in opposite phase to perform the compensation. The structure of a PV system connected to the grid presented in Fig.1.

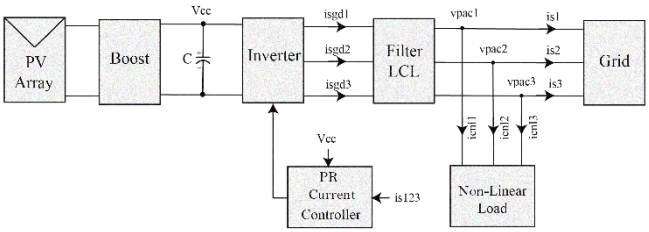

Figure 1. Structure of a PV connected to the electrical grid.

The PR controller is presented and discussed in [14-16]. The current controller can have a significant effect on quality of the current supplied to the grid and by the PV. Therefore, the controller provides a high quality sinusoidal output with minimal distortion to avoid harmonics. This controller is highly suitable for operating with sinusoidal references as the reference used in grid-connected PV inverters, making it an ideal solution for this application. The PR controller sets a gain at a certain frequency, in this case the resonant frequency, and there is almost no gain at the other frequencies.

Multiple harmonics of the fundamental frequency can be highlighted in the current and can be compensated for using additional PR controllers that act at particular harmonic frequencies to be reduced or eliminated. This compensation is used to reduce the harmonic distortion rate (THD), which must be less than 5% for systems with rated voltage between 120 and 69 kV and make the PV system compatible with the aforementioned norms and standards [14], [17]], [18]. This paper describes the PR design procedure and selective harmonic compensation applied for the 3rd, 5th, 7th, 11th through 25th. The current control and harmonic compensation design was carried out using the MATLAB/SIMULINK® platform. The PR simulation results at fundamental frequency and with additional harmonic compensation will be shown later. The platform developed for this article is a project of a three-phase PV with 6.5 kW of installed power connected to the electricity grid.

A. Filter LCL

The inductor-capacitor-inductor (LCL) is a type of third-order filter that is used when referring to PV structures connected to the electrical grid, allowing greater attenuation for higher-order harmonics, such as those produced by the inverter pulse width modulator (PWM). The LCL filter demonstrates some advantages when working in high power applications, as smaller size and lower cost inductors are needed to obtain a similar or better response to those obtained with the L or LC filter.

Fig.2 shows the relationship between current attenuation and frequency for an L, LC and an LCL filter, designed for the same working conditions. The LCL filter is intended to ensure that the current is sinusoidal, so the voltage harmonics generated by the PWM depend on the modulation index, the DC bus voltage and the PWM technique used. Note that resonance can lead the system to instability. Its effects can be minimized through active damping, using compensation loops in controllers using additional resistors, inductors or capacitors [19].

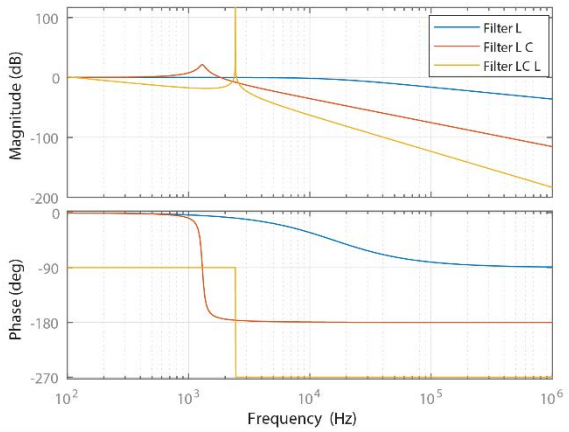

Figure 2. Bode diagram of the L, LC and LCL filters.

The transfer function of LCL filter is defined according to:

$$G_F(s) = \frac{1}{L_i s} \frac{\left(s^2 + s\left(\frac{R_d}{L_g}\right) + \left(\frac{1}{L_g C_f}\right)\right)}{\left(s^2 + s\left(\frac{(L_i + L_g)R_d}{L_i L_g}\right) + \left(\frac{L_i + L_g}{L_i L_g C_f}\right)\right)} \quad , (1)$$

L_i is the inverter side inductor, L_g is the grid side inductor, C_f is the filter capacitor and $R_d$is the damping resistance of the capacitor. The introduction of R_d in series with the capacitor C_f increases stability and reduces resonance [20].

This damping method is of the passive type. Although there are other passive and active damping methods, this damping method used was considered sufficient for the purpose of this article because it is simple.

where R_d is the damping resistors.

It should be noted the superiority of the LCL filter with regard to the attenuation of harmonic components produced at the switching frequency. According to the Bode diagram presented in Fig 2, it is observed that the LCL filter has a localized resonance. The filter resonance frequency is defined follows.

$$\omega_{res} = \sqrt{\frac{(L_i + L_g)}{L_i L_g C_f}}. \quad (2)$$

B. Controller PR

The PR controller is proposed as a regulator of sinusoidal signals introducing an infinite gain at the selected resonance frequency to eliminate the steady-state error of the signal at this frequency [21]. In Fig.4, the control loop of a PR controller similar to Fig 3 is shown. This controller is conceptually similar to a Proportional Integral (PI) Controller with high gain in DC direct current and guarantees a zero steady-state error for signals at this frequency [17].

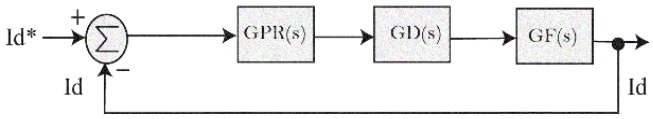

Figure 3. PR Controller loop block diagram.

The PR controller transfer function is defined as follows:

$$G_{PR}(s) = K_p + K_i \frac{s}{s^2 + {\omega_0}^2}, \quad (3)$$

where K_p is the proportional gain, K_i is the integral gain and ω_0 is the resonant frequency. The transfer function that represents a processing delay is defined follows:

$$G_D(s) = \frac{1}{1 + sT_s}, \quad (4)$$

where T_s is the period of a sample.

C. PR Controller with Harmonics Compensation

For this controller model, it is necessary to insert other PR controllers to perform the compensation of the specific harmonic. Fig.4 shows the control loop of a PR controller with harmonic compensation. The transfer function of the PR controller with harmonic compensation is defined as follows:

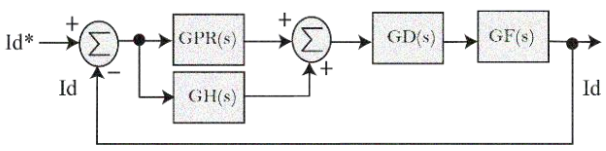

Figure 4. Block diagram of the PR controller loop with harmonics compensation.

$$G_H(s) = \sum_{h=3,5,7,9\ldots} K_{ih} \frac{s}{s^2 + (h\omega_0)^2}, \quad (5)$$

where K_{ih} is the Proportional gain and ω_0 is the resonant frequency, both specified for the specific harmonic.

III. LCL Filter and Resonant Proportional Comtroller Design

A. LCL Filter Design

The LCL filter is designed with the following specifications: the inverter side inductor L_i 1mH, the grid side inductor L_g 400μH, the filter capacitor C_f 15μ, and the damping resistance R_d 4.7Ω. Therefore, the transfer function shown in (1), results in:

$$G_F(s) = \frac{1}{10^{-3}s} \frac{(s^2 + 11750s + 1.7\ 10^8)}{(s^2 + 16450s + 2.33\ 10^8)}, \quad (6)$$

The resonance frequency ω_{res}, according to (2) it has a value of 15275 rad/s, 2.43kHz.

B. PR Controller Design

The PR controller was designed at the frequency ω_0 of 376.99 rad/s, 60Hz, the proportional gain K_p is 40.0 and the integral gain K_i is 6000.0 according to [22].

$$G_{PR}(s) = 40 + 6000 \frac{s}{s^2 + (2\pi 60)^2}, \quad (7)$$

For the PR controller to have optimal performance, the value of integral gain K_i has to be adjusted to a high value, so the steady-state error is as small as possible. The value of K_p is adjusted to obtain a frequency width sufficient to insert the other harmonic compensators without causing instability in the system.

C. PR Controller Design with Harmonics Compensation

The harmonic compensation PR controller is designed for the specific 5rd, 7th, 11th, 13th, 17th, 19th, 23th and 25th harmonics. A fine adjustment is performed on the compensators and the frequency ω_0 is established for each specific frequency. The proportional gain K_p is null and the integral gain K_i is 6000.0:

$$G_C(s) = G_{PR}(s) + \cdots + G_{25H}(s), \quad (8)$$

The harmonic compensator for the 5rd at frequency $5\omega_0$ is 1884.96 rad/s (300Hz). The harmonic compensator for the 7th at frequency $7\omega_0$ is 2638.94 rad/s (420Hz) and so on until the 25th at frequency $25\omega_0$ is 9424.78 rad/s (1500Hz). Each harmonic compensator is designed for its specific frequency and matched with the compensator at the fundamental frequency.

IV. PV System Implementation Methodology for Harmonic Compensation

A three-phase PV system connected to the electrical grid is presented in Fig. 1. The PV connection is carried out by means of a three-phase inverter to perform the following functions, such as active power injection and simultaneously assist in harmonic compensation.

A. Non – Linear Load

The non-linear load connected to the PCC consists of an uncontrolled rectifier feeding an r_L load. In this case, when these non-linear loads are connected to the PCC, the grid current is affected by harmonic distortion of the load non-linearities. When it comes to harmonic compensation, the DG can act as an active shunt filter by injecting harmonics in opposite phase to perform the compensation.

B. Voltage Control

The reference currents are obtained by measuring the current of the is_{123} grid. Control is implemented based on Vcc bus voltage, and is_{123}.The voltage control is responsible for providing the reference current Id^* as shown in Fig.3 and Fig.4. A maximum power point tracking algorithm (MPPT) based on Perturb & Observe (P&O) [23] was implemented, as shown in Fig.5

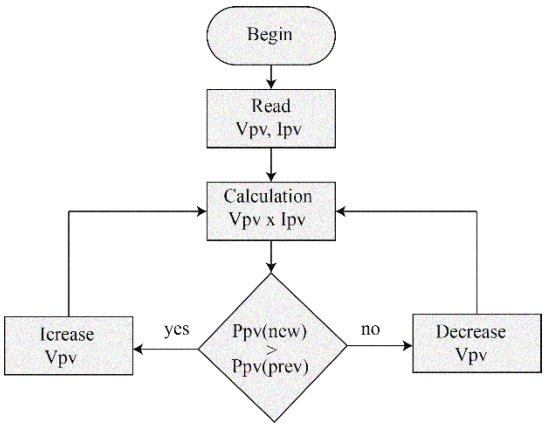

Figure 5. P&O Method (Perturb & Observe).

The difference between the reference voltage Vcc^* and Vcc generates an error that is processed by the controller (PI) and it generates the reference current Id^*in the synchronous reference, as shows in Fig.3 and Fig. .4 determining the energy balance of the system.

C. Current Control

The implementation of control strategy is carried out in the synchronous frame, using the Park *(abc-dq)* and Clarke *(abc-αβ)* transformation [22]. For a balanced system, the homopolar components are null. The control strategy consists of two cascade control systems, i.e, an internal current control to control the current in the is_{123} grid and an external voltage control to control the Vcc voltage bus, producing the reference currents for PWM modulation that PV system operates at maximum power. Fig.6 shows the block diagram of the current control strategy in detail.

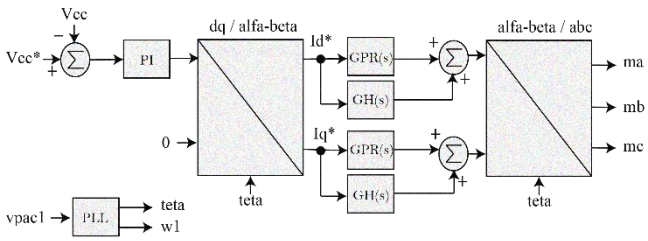

Figure 6. Block diagram of the complete control strategy.

TABLE 1. PARAMETERS PV ARRAY

Parameters	*Value*	*Unit*
V_{OC}	994	V
I_{SC}	8.69	A
V_{MPP}	806	V
I_{MPP}	8.07	A

V. RESULTS OF SIMULATIONS

Simulations were performed using software MATLAB/SIMULINK®, validating the control strategy and highlighting the harmonic compensation in the grid. Harmonic distortions were highlighted with regard to PQ problems. Table 2 shows the parameters used for simulation.

TABLE 2. SIMULATION PARAMETERS

Parameters	*Value*	*Unit*
Nominal Voltage (V_{grid})	127	V
Bus Voltage *(Vcc)*	750	V
Nominal Frequency (f_r)	60	Hz
Grid Inductance (L_g)	500	µH
Inverter Inductance (L_i)	1	mH
Filter Capacitor (C_f)	15	µF
Modulation Frequency (f_s)	10	kHz
Non- Linear Load (r_L)	60	Ω

In the grid, with a nominal frequency of 60 Hz, a PV array is connected through a three-phase inverter and a non-linear load of impedance r_L of 60 Ω which was represented by an uncontrolled rectifier with a purely resistive load. With the system in steady state, a load step is inserted in order to increase the power of the load connected to the PCC. The control strategy was implemented as shown in Fig.6. to carry out the control grid current is_{123} . Three cases were simulated:

- In the first case, the PV system is implemented providing active power, with non-linear load, without harmonic compensation;
- In the second case, the PV system is implemented providing active power, with non-linear load, performing harmonic compensation;
- In the third case, the PV system is implemented providing active power, with non-linear load variation, performing harmonic compensation.

A. First Case

A PV system without harmonic compensation is simulated. In this case, it is desired to inject a sinusoidal current into the controlled grid. The PR controller works in the mode without harmonic compensation, injecting only the power provided by the DG. Simulation results are presented in Fig.7, where the PCC voltage *(vpac1)*, load current *(icnl1)*, grid current *(is1)* and inverter current *(isgd1)* are shown.

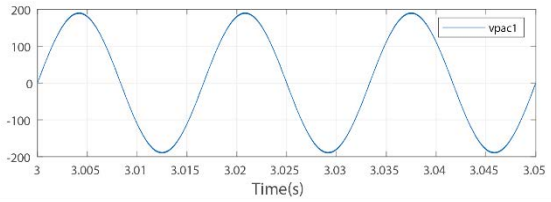

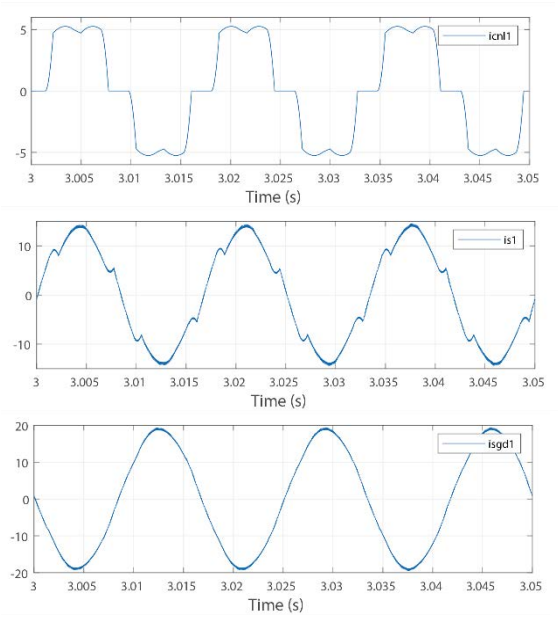

Figure 7. First Case – PCC voltage *(vpac1)*, load current *(icnl1)*, grid current *(is1)* and inverter current *(isgd1)*.

Fig.7 presents the voltage and current magnitudes of the DG connected to the grid. The grid current remains distorted due to the non-linear load being connected to the PCC with the THD of 24.94% and the inverter injects a sinusoidal current. The THD of the grid current, with the injection of active power by the DG, is 9.75%, degrading the power quality. The PCC voltage THD is 0.6% and the inverter current THD is 1.82%.

Fig.8, presents voltage magnitudes of the PCC and the controlled current of the grid. Even with the grid current degraded, they are in phase with a FP power factor of 0.97.

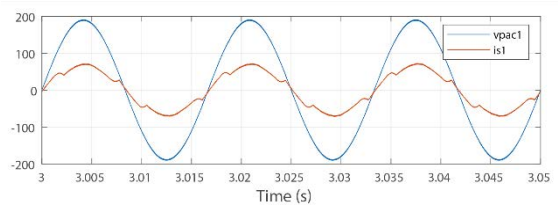

Figure 8. First Case – Voltage in the PCC *(vpac1)*, current in the grid *(is1)*.

In Fig.9, the frequency spectra of the voltage at the PCC *(vpac1)*, load current *(icnl1)*, current in the grid *(is1)* and the current in the inverter *(isgd1)* are presented.

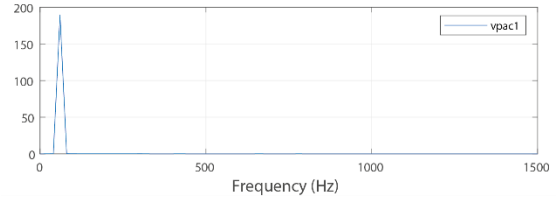

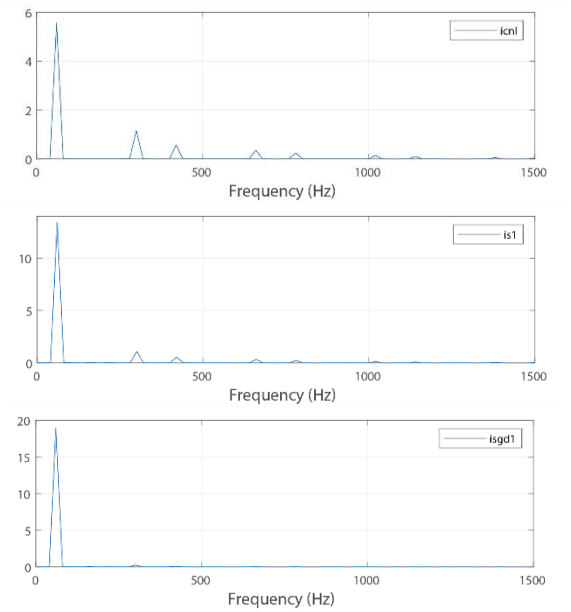

Figure 9. First Case – Frequency spectrum in the voltage at the PCC *(vpac1)*, load current *(icnl1)*, current in the grid *(is1)* and inverter current *(isgd1)*.

B. *Second Case*

The PV system is implemented providing active power, with non-linear load. The PR controller works by performing harmonic compensation. Simulation results are shown in Fig.10, where the PCC voltage *(vpac1)*, load current *(icn1l)*, grid current *(is1)* and inverter current *(isgd1)* are shown.

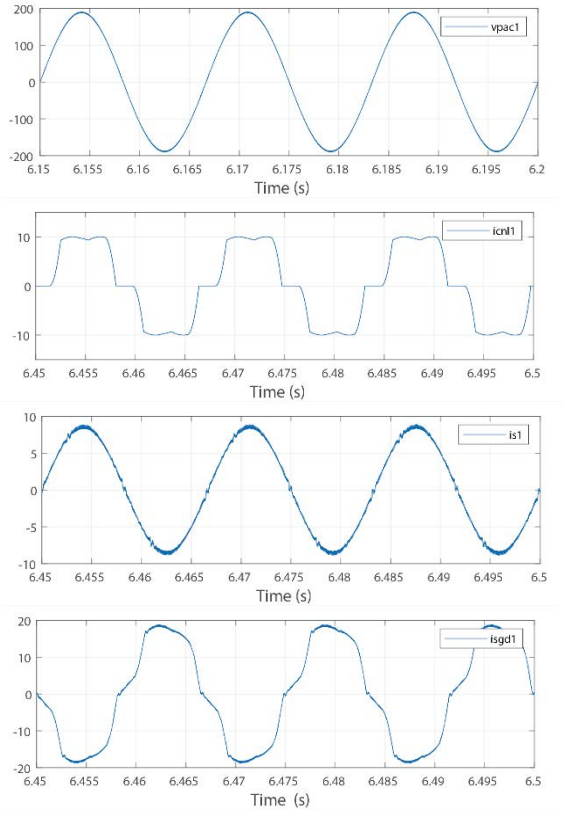

Figure 10. Second Case – PCC voltage *(vpac1)*, load current *(icnl1)*, grid current *(is1)* and inverter current *(isgd1)*.

The grid current is compensated even with the non-linear load connected to the PCC with the THD of 24.99% and the inverter injects an almost pure sinusoidal current. The THD of the main current, with active power injection by the DG, is 1.74%. The PCC voltage THD remains at 0.6% and the inverter current THD is around 7.45%. Fig.11 shows the voltage magnitudes of the PCC and the controlled current of the electrical grid. The grid current is not degraded and they are in phase with a PF power factor of 0.998.

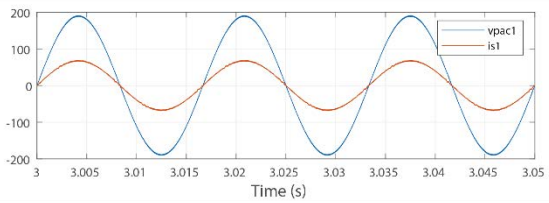

Figure 11. Second Case – Voltage in the PCC *(vpac1)*, grid current *(is1)*.

In Fig.12, the frequency spectrum of the voltage at the PCC *(vpac1)*, load current *(icnl1)*, current in the grid *(is1)* and the current in the inverter *(isgd1)* are presented.

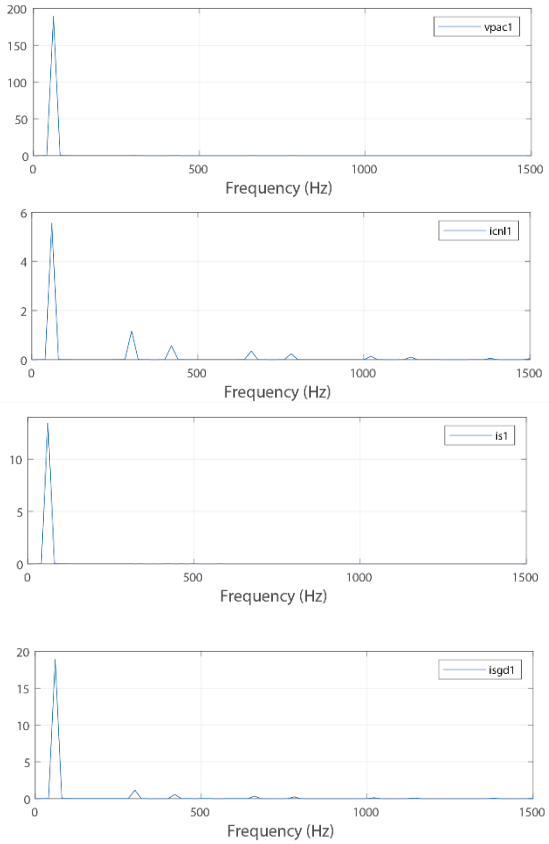

Figure 12. Second Case – Frequency spectrum in PCC voltage *(vpac1)*, load current *(icnl1)*, current grid *(is1)* , inverter current *(isgd1)*.

C. *Third Case*

In the third case, the PV system is implemented providing active power, with non-linear load and at time t = 6 s a load step of 50% was applied, in order to double the load power. The simulation results are presented in Fig.13, where the PCC voltage *(vpac1)*, load current *(icnl1)*, grid current *(is1)* and inverter current *(isgd1)* are shown when load step is applied.

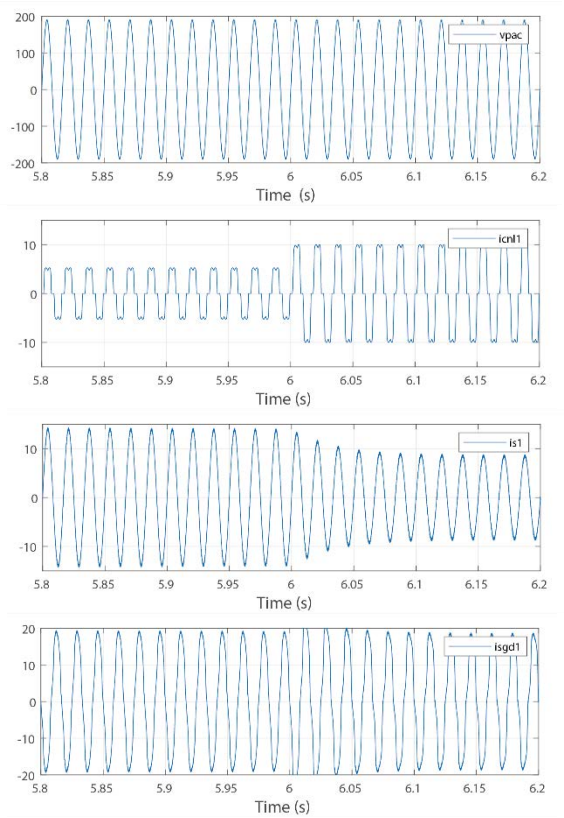

Figure 13. Third Case – Load Step - PCC voltage *(vpac1)*, load current *(icnl1)*, grid current *(is1)* and inverter current *(isgd1)*.

After the load step, simulation results are presented in Fig.14, where the PCC voltage *(vpac1)*, load current *(icnl1)*, grid current *(is1)* and inverter current *(isgd1)* are shown.

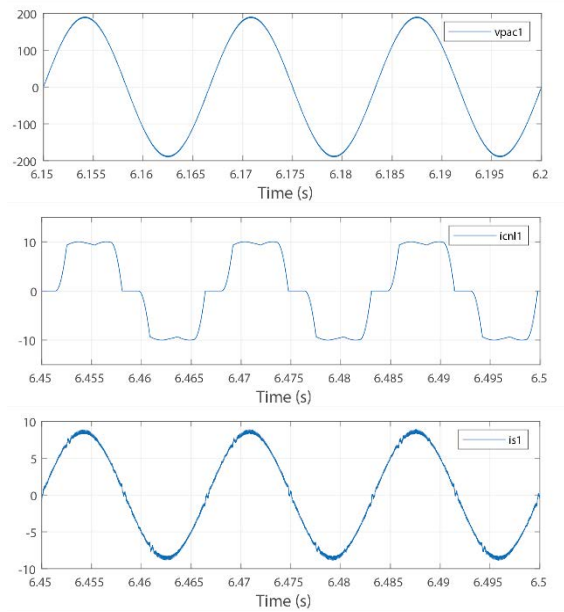

The grid current is compensated even with the non-linear load connected to the PCC with the THD of 22.16% and the inverter injects an almost pure sinusoidal current.

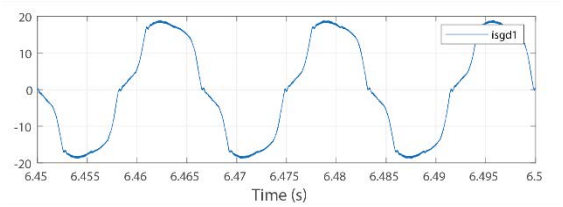

Figure 14. Third Case – PCC voltage *(vpac1)*, load current *(icnl1)*, grid current *(is1)* and inverter current *(isgd1)*.

The THD of the main current, with the active power injection by the DG, is 2.94%. The PCC voltage THD remains at 0.6% and the inverter current THD is around 12.43%.

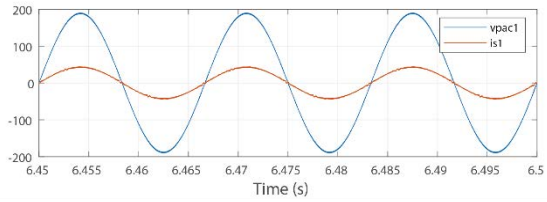

Figure 15. Third Case – Voltage in the PCC *(vpac1)*, current in the grid *(is1)*.

In Fig.16, the frequency spectra of the voltage at the PCC *(vpac1)*, load current *(icnl1)*, current grid *(is1)* and current inverter *(isgd1)* are presented.

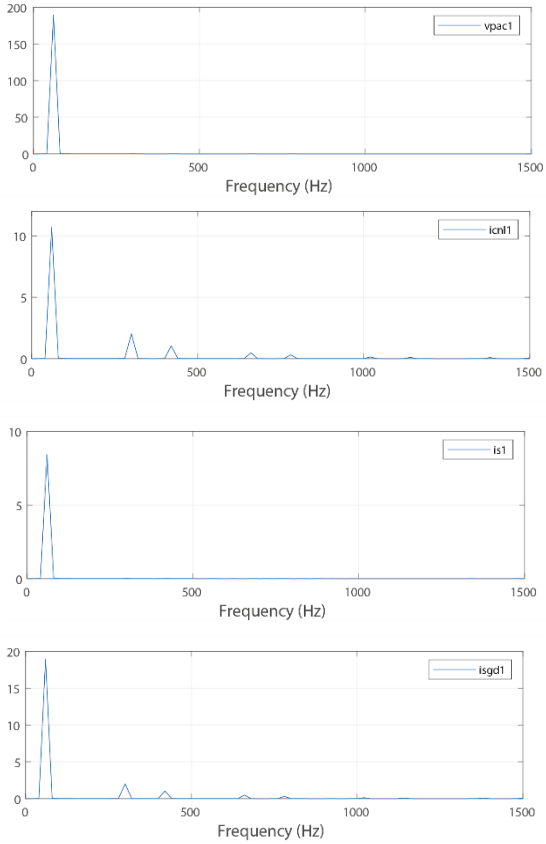

Figure 16. Third Case – Frequency spectrum in the voltage at the PCC *(vpac1)*, load current *(icnl1)*, current grid *(is1)* and current inverter *(isgd1)*.

In Table 3, the THD of the controlled current of the electrical grid and of the non-linear load for the sceneries described are shown.

TABLE 3. CURRENT AND NON-LINEAR THD

Case	*THD (%)*	
	is1	***icnl1***
1	9.75	24.94
2	1.74	24.99
3	2.94	22.16

VI. CONCLUSIONS

This paper presented harmonic compensation in PV systems connected to the electrical grid, in order to mitigate harmonics from non-linear loads in the PCC. For the simulations, a PV system was implemented in the electrical grid, as well as control strategies based on power flow, whose currents had harmonic components of non-linear load currents.

The implemented control strategies have positive characteristics as they require less computational effort and do not require the harmonics detection process, showing efficient in the injection of active power and in the harmonics compensation. In the simulations, the harmonic compensation in PV systems connected to the electrical grid can be performed by means of a three-phase inverter. Without harmonic compensation, the inverter injects a sinusoidal current added to the distorted current drained by the load into the PCC, with harmonic current circulating through the grid. In this case, in the first, a harmonic content of an average of 0.6% and 9.75%, voltage and current, and a power factor of 0.97 were obtained at the coupling point. In the second case, with the harmonics compensation, a harmonic content of an average of 0.6% and 1.74%, voltage and current, and a power factor of 0.99, practically unity, was obtained at the coupling point. In the third case, even with the increase in non-linear load power, a harmonic content of 0.6% and 2.94%, voltage and current, and a power factor of 0.97. Therefore, the three-phase inverter was able to supply active power from the photovoltaic system to the load, compensating harmonics from the non-linear load, as well as the control strategy, mitigating the harmonics from the load. For future work, this paper proposes on modeling the EAF as an industrial non-linear load, so that can perform harmonics and interharmonics compensation.

ACKNOWLEDGEMENT

This paper is supported by Coordenação de Aperfeiçoamento de Pessoal de Nível Superior (Capes/Proex). The authors also thank Companhia Hidro Elétrica do São Francisco (Chesf) for the technical and financial support of this research in the R&D+I Project entitled Optimization of Renewable Power Systems with High Performance Storage (Oseraad), that is a cooperation between Chesf and Federal University of Campina Grande (R&D+I-0048-0317/2020).

REFERENCES

[1] Aneel (2022). Superintendência de Concessões e Autorizações de Geração (SCG): Geração Distribuída. Agência Nacional de Energia Elétrica.

[2] Santoso, S., McGranaghan, M., Dugan, R., & Beaty, H. (2012). *Electrical power systems quality*. McGraw-Hill Education.

[3] Henderson, R. D., & Rose, P. J. (1994). Harmonics: the effects on power quality and transformers. *IEEE transactions on industry applications*, *30*(3), 528-532.

[4] Watson, N. R., Scott, T. L., & Hirsch, S. J. (2009). Implications for distribution networks of high penetration of compact fluorescent lamps. *IEEE transactions on power delivery*, *24*(3), 1521-1528.

[5] Akagi, H. (2005). Active harmonic filters. *Proceedings of the IEEE*, *93*(12), 2128-2141.

[6] Chilipi, R., Al Sayari, N., Al Hosani, K., & Beig, A. R. (2016). Control scheme for grid-tied distributed generation inverter under unbalanced and distorted utility conditions with power quality ancillary services. IET Renewable Power Generation, 10(2), 140-149.

[7] Campanhol, L. B., da Silva, S. A. O., Sampaio, L. P., & Azauri, A. O. (2013, October). A grid-connected photovoltaic power system with active power injection, reactive power compensation and harmonic filtering. In *2013 Brazilian Power Electronics Conference* (pp. 642-649). IEEE.

[8] Belaidi, R., Fathi, M., Larafi, M. M., Kaci, G. M., & Haddouche, A. (2015, December). Power quality improvement based on shunt active power filter connected to a photovoltaic array. In *2015 3rd International Renewable and Sustainable Energy Conference (IRSEC)* (pp. 1-6). IEEE.

[9] Zammit, D., Staines, C. S., Apap, M., & Licari, J. (2017). Design of PR current control with selective harmonic compensators using Matlab. *Journal of Electrical Systems and Information Technology*, *4*(3), 347-358.

[10] Akagi, H., Kanazawa, Y., & Nabae, A. (1984). Instantaneous reactive power compensators comprising switching devices without energy storage components. IEEE Transactions on industry applications, (3), 625-630.

[11] F II, I. (1993). IEEE recommended practices and requirements for harmonic control in electrical power systems. *New York, NY, USA*, 1-1.

[12] IEEE 929 2000 Recommended Practice for Utility Interface of Photovoltaic (PV) Systems.

[13] IEC 61727 2004 Standard Photovoltaic (PV) Systems-Characteristics of the Utility Interface.

[14] Teodorescu, R., Blaabjerg, F., Borup, U., Liserre, M., 2004. A new control structure for grid-connected LCL PV inverters with zero steady-state error and selective harmonic compensation. In: APEC'04 Nineteenth Annual IEEE Conference, California.

[15] Liserre, M., Teodorescu, R., Chen, Z., 2005a. Grid Converters and Their Control in Distributed Power Generation Systems. IECON 2005 Tutorial.

[16] Ciobotaru, M., Teodorescu, R., Blaabjerg, F., 2005. Control of a Single-Phase PV Inverter. EPE2005, Dresden

[17] Teodorescu, R., Blaabjerg, F., Liserre, M., Loh, P.C., 2006. Proportional-resonant controllers and filters for grid-connected voltage-source converters. IEEE Proc. Electr. Power Appl. 153 (5)

[18] Castilla, M., Miret, J., Matas, J., de Vicuna, L.G., Guerrero, J.M., 2009. Control design guidelines for single-phase grid-connected photovoltaic inverters with damped resonant harmonic compensators. IEEE Trans. Ind. Power Electron. 56 (11).

[19] Caracas, J. V. M. (2013). Avaliação das estratégias de controle e projeto de inversores para conexão de fontes fotovoltaicas à rede CA.

[20] Pradeep, V., Kolwalkar, A., Teichmann, R., 2004. Optimized Filter Design for IEEE 519 Compliant Grid Connected Inverters. IICPE 2004, Mumbai, India.

[21] [21] Zmood, D. N., Holmes, D. G., & Bode, G. (1999, October). Frequency domain analysis of three phase linear current regulators. In *Conference Record of the 1999 IEEE Industry Applications Conference. Thirty-Forth IAS Annual Meeting (Cat. No. 99CH36370)* (Vol. 2, pp. 818-825). IEEE.

[22] Timbus, A. V., Ciobotaru, M., Teodorescu, R., & Blaabjerg, F. (2006, March). Adaptive resonant controller for grid-connected converters in distributed power generation systems. In *Twenty-First Annual IEEE Applied Power Electronics Conference and Exposition, 2006. APEC'06.* (pp. 6-pp). IEEE.

[23] Faranda, R., & Leva, S. (2008). Energy comparison of MPPT techniques for PV Systems. *WSEAS transactions on power systems*, *3*(6), 446-455.

[24] Han, Y., Luo, M., Zhao, X., Guerrero, J. M., & Xu, L. (2015). Comparative performance evaluation of orthogonal-signal-generators-based single-phase PLL algorithms—A survey. *IEEE Transactions on Power Electronics*, *31*(5), 3932-3944.